



Open Access : : ISSN 1847-9286

[www.jESE-online.org](http://www.jESE-online.org)

Original scientific paper

## Electrochemical study of doped $\text{LiFePO}_4$ as a cathode material for lithium-ion battery

Andrey Chekannikov<sup>\*,\*\*,\*</sup>, Svetlana Novikova<sup>\*\*\*</sup>, Tatiana Kulova<sup>\*\*</sup>, Alexander Skundin<sup>\*\*</sup>, Andrey Yaroslavtsev<sup>\*\*\*</sup>

<sup>\*</sup>Skolkovo Institute of Science and Technology, 100 Novaya str., Skolkovo, Odintsovsky district, 143025 Moscow Region, Russia

<sup>\*\*</sup>A.N. Frumkin Institute of Physical chemistry and Electrochemistry of the Russian Academy of Sciences, 31-4 Leninsky prospect, 119071 Moscow, Russia

<sup>\*\*\*</sup>Kurnakov Institute of General and Inorganic Chemistry of the Russian Academy of Sciences, 31 Leninsky prospect, 11999 Moscow, Russia

✉ Corresponding Author: [andrey.chekannikov@skolkovotech.ru](mailto:andrey.chekannikov@skolkovotech.ru);

Received: October 1, 2015; Revised: December 17, 2015; Accepted: February 4, 2016

---

### Abstract

$\text{LiFe}_{1-x}\text{V}_x\text{PO}_4/\text{C}$  ( $x = 0.01, 0.03, 0.05, 0.1$ ) composites had been obtained by sol-gel method and characterized with the use of the XRD-analysis, SEM and charge/discharge tests. The doping was shown to result in decrease of electrode polarization, and correspondingly in capacity increase at high C-rates.

### Keywords

Cathode materials; Lithium ion battery; Lithium iron phosphate; Vanadium doping

---

### Introduction

Since the first report on olivine lithium iron phosphate (LFP) in 1997 [1] this substance became the most recent state-of-the-art material of positive electrodes of lithium-ion batteries. The theoretical specific capacity of  $\text{LiFePO}_4$  is  $170 \text{ mA h g}^{-1}$  and electrodes based on  $\text{LiFePO}_4$  demonstrate a flat voltage plateau of around 3.45 V (vs.  $\text{Li}/\text{Li}^+$ ). Rather low electronic conductivity ( $\sigma \approx 10^{-9} \text{ S cm}^{-1}$ ) should be mentioned as one of the disadvantages of this material. However, electron transfer can be enhanced by a simple carbon coating of the LFP particles *in situ* during synthesis or *ex situ* by post-treatment. This leads to significant increase of the achievable specific capacity. Different ways for further improvement of this active material have been extensively studied for the last few years: *i*) development of advanced nanostructured LFP-carbon composites;

ii) replacement of carbon by conductive, electrochemically active polymers; iii) doping of LFP by the ions of transition metals and so on. In particular, LFP doping with vanadium has been suggested as a way for the increase in mobility and diffusion coefficient of Li<sup>+</sup> ions due to lattice expansion and Li–O interaction weakening [2]. The authors of [3] have studied the structure and properties of LiFe<sub>0.9</sub>V<sub>0.1</sub>PO<sub>4</sub> and found that the cathode properties of doped counterpart, including reversible capacity, cycleability and rate capability are better than those of LiFePO<sub>4</sub>. Later the lengthening and weakening of Li–O bond and improvement of the electrochemical performance especially under the high C rate were confirmed by the examples of LiFe<sub>0.95</sub>V<sub>0.05</sub>PO<sub>4</sub> [4], LiFe<sub>0.97</sub>V<sub>0.03</sub>PO<sub>4</sub> [5] and LiFe<sub>0.99</sub>V<sub>0.01</sub>PO<sub>4</sub> [6]. Intriguingly, even 0.32 wt.% V atoms substituted for some Fe atoms can notably improve the cathode property. The authors of [7] have systematically studied a series of materials LiFe<sub>1-x</sub>V<sub>x</sub>PO<sub>4</sub> with 0 ≤ x ≤ 0.13. They found that in the whole concentration range, the chemical valence of Fe<sup>2+</sup> remains invariant whereas the valence of vanadium evolves from +4 to +3. It was found also that the phase composition varies with the adding amount. The materials with 0 ≤ x < 0.08 are single-phase, and materials with x > 0.08 are two-phase, properties and electrochemical behavior of both kinds of materials being different. The electrical conductivity as well as the diffusion coefficient in single-phase region are enhanced with “x” increase. Upon going into two-phase region, the both quantities plummet down. Close results were reported in [8]. Recently, the influences of adding vanadium to the structure evolution and electrochemical performance of LiFePO<sub>4</sub> are systematically investigated by *in-situ* X-ray powder diffraction and X-ray absorption near edge structure spectroscopy in [9]. The results indicate that the addition of a small amount of vanadium (less than at 1 %) significantly reduces the formation of non-crystalline (highly disordered) triphylite and remnant heterosite phases in the cathode of battery especially at the rate capability higher than 0.5C. The cycle stability of LiFePO<sub>4</sub> cathode with vanadium additive after 80 cycles retains higher by 14.9 % compared to that without vanadium additive. Such an enhancement could be attributed to the ion diffusion kinetics being improved and inactive triphylite being reduced by the supervalent-vanadium additive in cathode during electrochemical redox cycles.

In present work, LFP doped with vanadium was studied. The composition of samples studied is LiFe<sub>1-x</sub>V<sub>x</sub>PO<sub>4</sub>/C, where x = 0.01, 0.03, 0.05, 0.1, therefore vanadium ions partially substituted for iron ions.

## Experimental

LiFe<sub>1-x</sub>V<sub>x</sub>PO<sub>4</sub>/C (x = 0.01, 0.03, 0.05, 0.1.) composite materials coated with fine carbon layer were prepared by a sol–gel process described elsewhere [5,10]. The LiNO<sub>3</sub>, Fe(NO<sub>3</sub>)<sub>3</sub>·9H<sub>2</sub>O, NH<sub>4</sub>VO<sub>3</sub>, NH<sub>4</sub>H<sub>2</sub>PO<sub>4</sub> and sucrose were used as starting materials. The resulting precursor was finally calcined at 650 °C for 10 h in an argon atmosphere. Carbon converted from sucrose acted as reducing and conducting agent and its amount was ~5 wt. % in the final product according to the TGA data.

Crystal structure was characterized by X-ray diffraction (XRD) with CuK<sub>α</sub> radiation performed on a Rigaku D/MAX 2200 diffractometer. XRD data were analyzed using Rigaku Application Data Processing software. Microstructures of obtained materials were examined with the help of the scanning electron microscope Carl Zeiss NVision 40. Electrode paste was prepared by thoroughly mixing 85 % LiFe<sub>1-x</sub>V<sub>x</sub>PO<sub>4</sub>/C as an active material, 10 % conductive carbon black (Timcal, Belgium), and 5 % binder (polyvinylidene fluoride (Aldrich) dissolved in anhydrous N-methyl-2-pyrrolidinone

(Aldrich,  $\leq 50$  ppm  $\text{H}_2\text{O}$ ). The paste was applied to stainless steel gauze (current collector) as a  $15 \text{ mg/cm}^2$  layer. The resultant electrode was pressed at 100 MPa and vacuum-dried at  $120^\circ\text{C}$  for 8 h.

Electrochemical tests were performed in hermetically sealed three-electrode ( $\text{LiFe}_{1-x}\text{V}_x\text{PO}_4/\text{C}/\text{Li}/\text{Li}$ ) cells. The area of the working electrode was  $2.25 \text{ cm}^2$ , and that of the auxiliary (lithium) electrode was  $5 \text{ cm}^2$ . The cells were assembled in a glove box under an argon atmosphere with a humidity of  $<10$  ppm. A nonwoven polypropylene separator (NPO Ufim, Russia) was placed between electrodes. 1 M  $\text{LiPF}_6$  solution in a mixture of ethylene carbonate, diethyl carbonate and dimethyl carbonate (1:1:1) was used as electrolyte. The water content in the electrolyte, measured by a method of a Fischer coulometric titration, was equal to 20 ppm. Electrochemical cycling of the cells was performed at voltages range 2.5 - 4.3 V using a ZRU 50 mA-10 V charge-discharge system (Buster, Russia). Certain experiments were carried out with using of more power device, specifically, ZRU 5 A-18 V (Buster, Russia). The tests were performed in galvanostatic mode at a currents densities of 20, 100, 200, 400, 800, 1600, 3200 mA/g.

## Results and discussion

### XRD

Fig. 1 shows the XRD pattern for  $\text{LiFe}_{1-x}\text{V}_x\text{PO}_4$  ( $x = 0.01, 0.03, 0.05, 0.1$ ). All materials obtained have olivine structure and are indexed in the orthorhombic  $Pnma$  space group.  $\text{LiFePO}_4$  doping with V results in slight changes in unit cell sizes

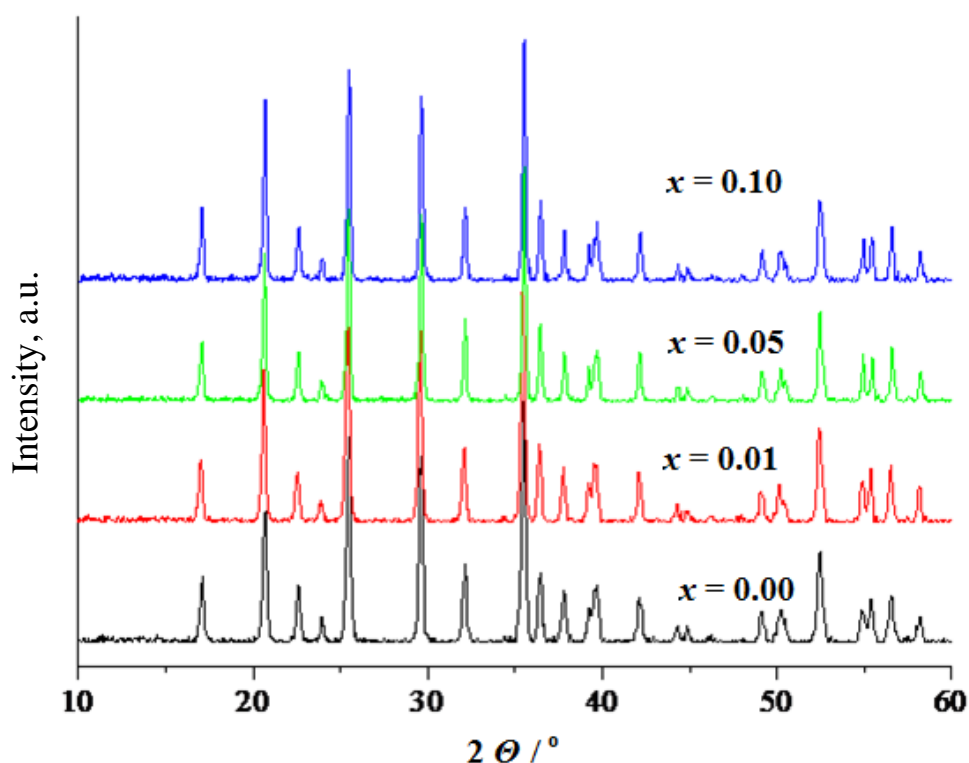


Figure 1. XRD pattern of  $\text{LiFe}_{1-x}\text{V}_x\text{PO}_4/\text{C}$

When comparing  $\text{LiFe}_{1-x}\text{V}_x\text{PO}_4$  with  $\text{LiFePO}_4$ , the  $a$  and  $c$  axes change is within the error, while  $b$  axis shrinks from  $0.6007 \pm 0.0002 \text{ nm}$  for  $\text{LiFePO}_4$  to  $0.5997 \pm 0.0002 \text{ nm}$  for  $\text{LiFe}_{0.9}\text{V}_{0.1}\text{PO}_4$ . That is in agreement with results reported in literature according to which a slight decrease in volume cell value is observed for V-doped  $\text{LiFePO}_4$  [7,11,12]. At the same time, one can see that XRD pattern

for  $\text{LiFe}_{0.9}\text{V}_{0.1}\text{PO}_4/\text{C}$  does not differ from other patterns, and therefore there are no evidences of two-phase nature of this material. This result contradicts the data of [7].

It should be noted that no diffraction peaks from impurities or residual carbon were detected. This fact is no wonder because heat treatment at  $650^\circ\text{C}$  resulted in carbonization with formation of non-crystalline matter.

According to XRD data the mean size of X-ray coherent scattering regions for the investigated samples varies in the range 33 to 43 nm.

### SEM

Electron microscopy data have shown that the average size of the  $\text{LiFePO}_4/\text{C}$  particles is consistent with the coherent scattering regions and amounts to  $\sim 40$  nm. The aggregation of the particles was observed for V-doped samples. The particle size of  $\text{LiFe}_{1-x}\text{V}_x\text{PO}_4/\text{C}$  samples has a wide distribution range from 100 nm to more than  $2\ \mu\text{m}$  according to SEM data (Fig. 2).

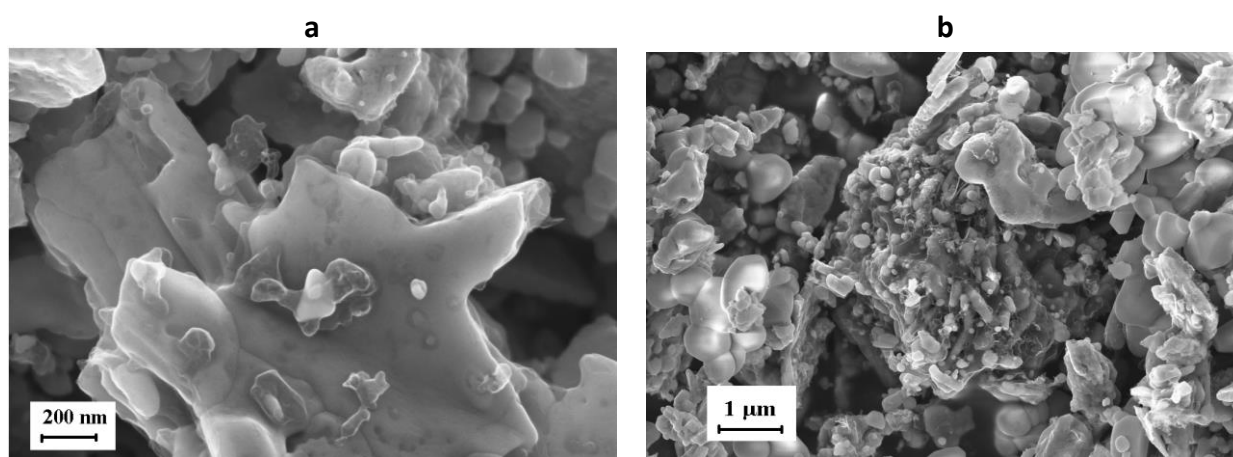


**Figure 2.** SEM microphotographs of  $\text{LiFe}_{0.99}\text{V}_{0.01}\text{PO}_4/\text{C}$  at different magnifications (a,b).

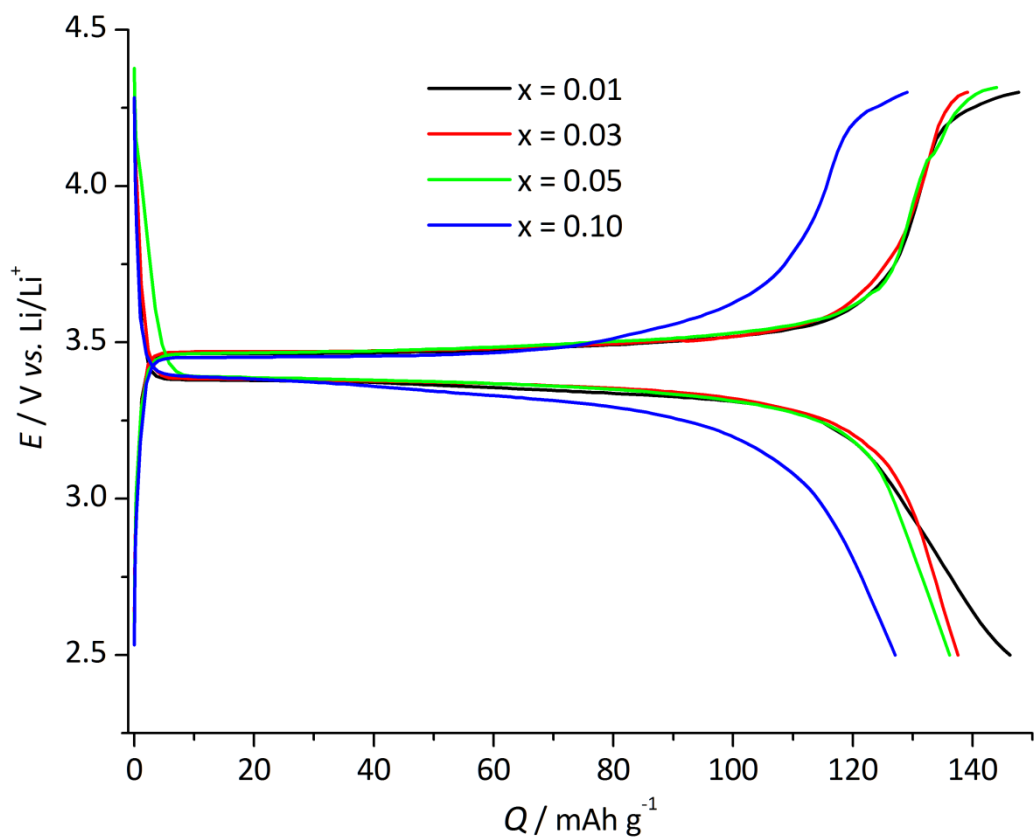
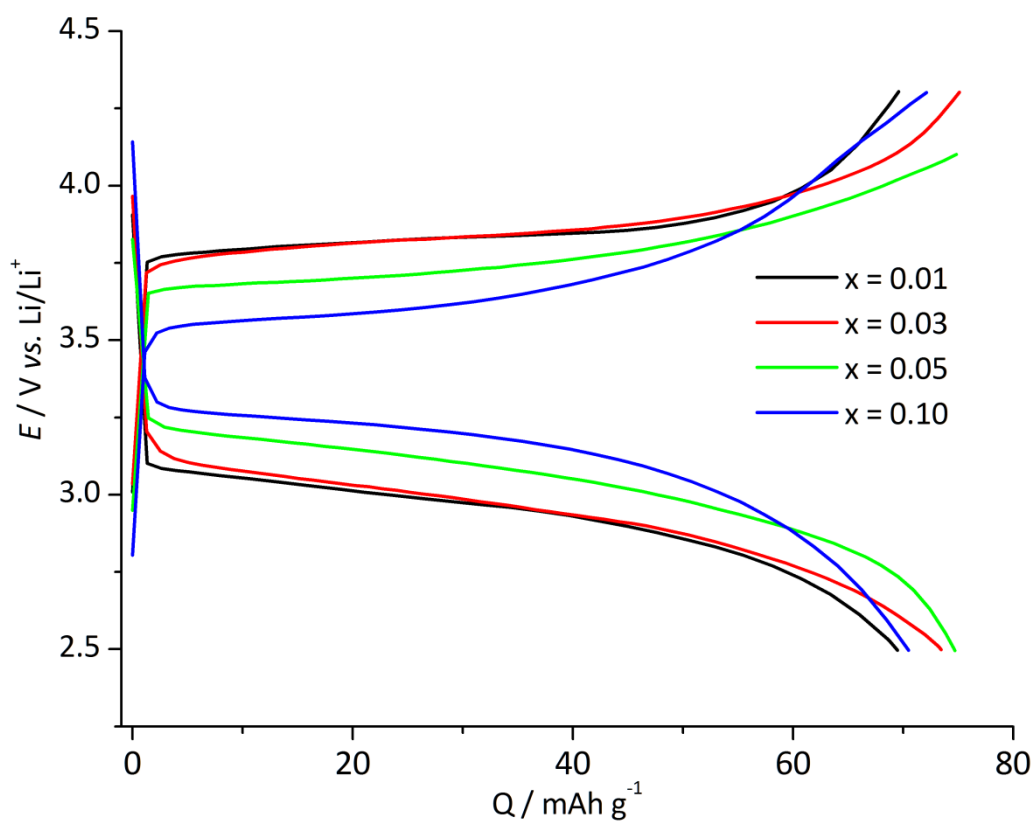
### Charge/discharge behavior

The charge-discharge curves of various samples at current density  $20\ \text{mA g}^{-1}$  (what corresponded about C/8 rate) to a cutoff voltage between 2.5 and 4.3 V are shown in Fig. 3a. One can see that the curves for all samples with  $x = 0.01, 0.03,$  and  $0.05$  coincide. The electrode with  $\text{LiFe}_{0.9}\text{V}_{0.1}\text{PO}_4$  demonstrates slightly less capacity. These results agree with data of [7] in spite of the fact that all materials were single phase.

Increase in current density results in increase of electrode polarization, and this increase depends on doping level: the higher doping level, the less polarization increase. This result also agrees with conductivity enhancement along with doping. Fig. 3b shows the charge-discharge curves at current density  $400\ \text{mA g}^{-1}$  (what corresponded about 2.5 C rate).

A half of difference between average potential of anodic and cathodic processes  $\delta E$  could present some generalized value of polarization. Fig. 4a shows dependence of  $\delta E$  on current density  $j$  for all samples studied. The dependence of  $\delta E$  on  $j^{1/2}$  is shown in Fig. 4b. The latter plots are almost linear that is typical for the systems with distributed parameters, in which the polarization has diffusion and ohmic nature. Surely, the data obtained in the present work do not allow discrimination of both factors (diffusion and ohmic). Figs. 4a and 4b vividly show the effect of doping upon electrode polarization.

a

**b**

**Figure 3.** Charge-discharge curves for  $\text{LiFe}_{1-x}\text{V}_x\text{PO}_4$  ( $x = 0.01, 0.03, 0.05, 0.1$ ):  
**a** - Current density  $20 \text{ mA g}^{-1}$ ; **b** - Current density  $400 \text{ mA g}^{-1}$

Fig. 5 presents the results of charge/discharge cycling with different current densities. It is worth noting that at rather low C rates the capacity of slightly doped samples exceeds that of heavy doped materials. At high C rates this ratio changes due to notable decrease in polarization for heavy doped samples. Indeed, at current density 20 mA g<sup>-1</sup> the discharge capacity of LiFe<sub>1-x</sub>V<sub>x</sub>PO<sub>4</sub> is equal to 146, 139, 132, and 128 mAh g<sup>-1</sup> for x = 0.01, 0.03, 0.05 and 0.1, correspondingly. At 1600 mAh g<sup>-1</sup> discharge capacity of the same samples was 24, 28, 29 and 39 mAh g<sup>-1</sup>.

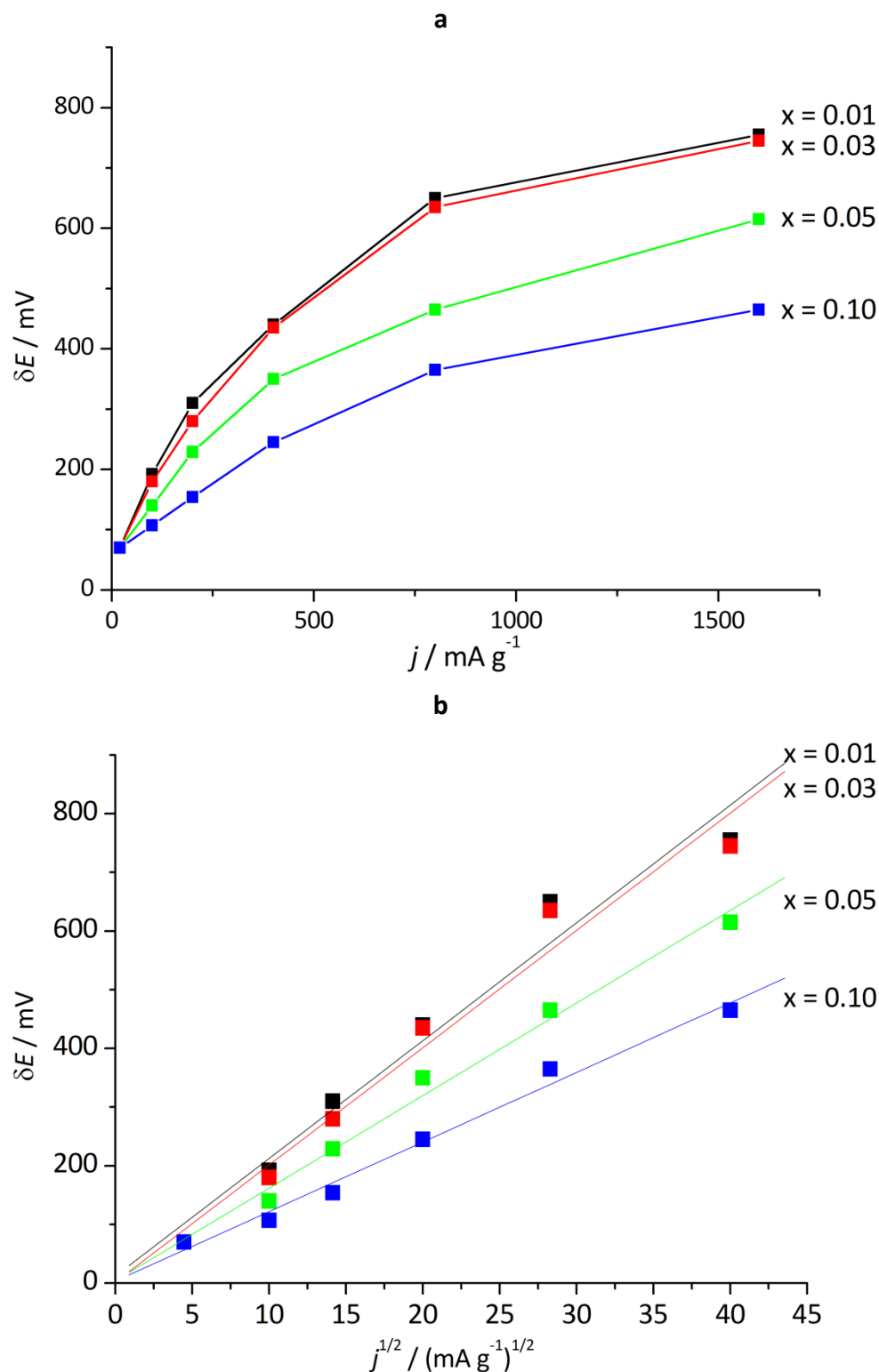


**Figure 4.** **a** - Electrode polarization vs. current density for doped LFP; **b** - Electrode polarization vs. square root of current density for doped LFP. The straight lines are drawn by minimal squares method

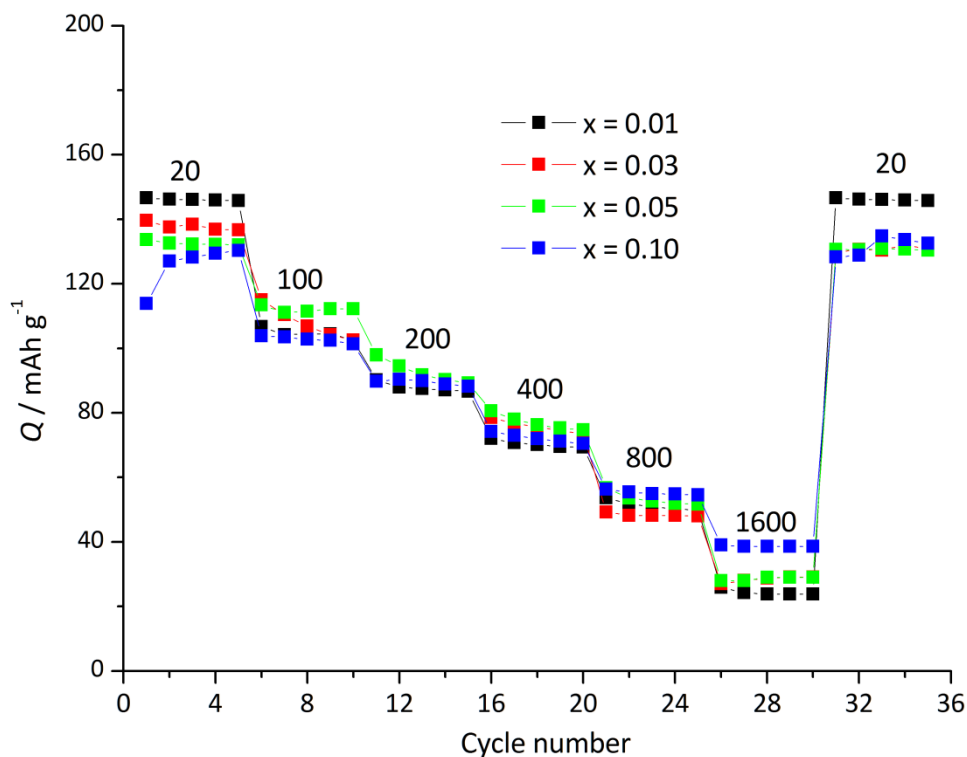


**Figure 5.** Cycling performances of doped LFP cathodes measured with different rates in the voltage range of 2.5–4.3V

## Conclusion

Lithium iron phosphate doped with vanadium ( $\text{LiFe}_{1-x}\text{V}_x\text{PO}_4$  with  $x = 0.01, 0.03, 0.05,$  and  $0.1$ ) and covered by fine carbon was synthesized by a sol-gel method from  $\text{LiNO}_3, \text{Fe}(\text{NO}_3)_3 \cdot 9\text{H}_2\text{O}, \text{NH}_4\text{VO}_3, \text{NH}_4\text{H}_2\text{PO}_4$  and sucrose as starting materials. XRD investigation showed that materials obtained have olivine structure and are indexed in the orthorhombic  $Pnma$  space group.  $\text{LiFePO}_4$  doping with V results in slight changes in unit cell sizes. Electron microscopy data have shown that the average size of the  $\text{LiFe}_{1-x}\text{V}_x\text{PO}_4/\text{C}$  primary particles amounts to  $\sim 40$  nm. At rather low C rates the capacity of slightly doped samples amounts to 146 mAh/g and exceeds that of heavy doped materials. At high C rates this ratio changes due to notable decrease in polarization for heavy doped samples.

**Acknowledgement:** The present work is supported by the Russian Foundation for Basic Research (Grant № HK 14-29-04068).

## References

- [1] A.K. Padhi, K.S.Nanjundaswamy, J.B.Goodenough, *J. Electrochem. Soc.* **144** (1997) 1188–1194.
- [2] D. Wang, H. Li, S. Shi, X. Huang, L. Chen, *Electrochim. Acta* **50** (2005) 2955–2958.
- [3] Y. Wen, L. Zeng, Z. Tong, L. Nong, W. Wei *J. Alloys Compd.* **416** (2006) 206–208.
- [4] Mu-Rong Yang and Wei-Hsin Ke. *J. Electrochem. Soc.* **155** (2008) A729-A732.
- [5] C.S. Sun, Z. Zhou, Z.G. Xu, D.G. Wang, J.P. Wei, X.K. Bian, J. Yan *J. Power Sources* **193** (2009) 841–845.
- [6] H. Liu, C. Li, Q. Cao, Y. P. Wu, R. Holze. *J. Solid State Electrochem.* **12** (2008) 1017-1020.
- [7] J. Ma, B. Li, H. Du, C. Xu, F. Kang *J. Electrochem. Soc.* **158** (2011) A26–A32.



- [8] Mao–Sung Chen, She–huang Wu, Wei Kong Pang, *J. Power Sources* **241** (2013) 690–695.
- [9] Chih-Wei Hu, Tsan-Yao Chen, Kai-Sheng Shih, Pin-Jiun Wu, Hui-Chia Su, Ching-Yu Chiang, An-Feng Huang, Han-Wei Hsieh, Chia-Chin Chang, Bor-Yuan Shew, Chih-Hao Lee, *J. Power Sources* **270** (2014) 449-456.
- [10] D. V. Safronov, S. A. Novikova, T. L. Kulova, A. M. Skundin, and A. B. Yaroslavtsev. *Inorganic Materials* **48** (2012) 513–519.
- [11] Ming Chen, Leng-Leng Shao, Hua-Bin Yang, Tie-Zhen Ren, Gaohui Du, Zhong-Yong Yuan, *Electrochim. Acta* **167** (2015) 278–286.
- [12] Lu-Lu Zhang, Gan Liang, A. Ignatov, M. C. Croft, Xiao-Qin Xiong, I-Ming Hung, Yun-Hui Huang, Xian-Luo Hu, Wu-Xing Zhang, and Yun-Long Peng. *J. Phys. Chem. C* **115** (2011) 13520–13527.